J. Plasma Phys. (2022), *vol*. 88, 905880118
Published by Cambridge University Press
doi:10.1017/S0022377822000058

Generation of the fluctuations by a charged dust beam in the ionosphere

Lin Wei[1], **Bo Liu**[1], **Heng Zhang**[1],† **and Wen-Shan Duan**[1],†

[1]College of Physics and Electronic Engineering, Northwest Normal University, Lanzhou 730070, PR China

(Received 20 October 2021; revised 12 January 2022; accepted 12 January 2022)

Different kinds of waves and instabilities in the F-region of the ionosphere excited by the relative streaming of the dust beam to the background plasma are studied in the present paper. The dispersion relations of different waves are obtained on different time scales. It is found from our numerical results that there are both a stable upper hybrid wave on the electron vibration time scale and a stable dust ion cyclotron wave on the ion vibration time scale. However, the chaotic behaviour appears on the dust particles vibration time scale due to the relative streaming of the dust particles to the background plasma. Such instabilities may drive plasma irregularities that could affect radar backscatter from the clouds.

Keywords: dusty plasmas, plasma simulation, plasma waves

1. Introduction

In recent years, research on rocket exhaust plumes has gained more attention owing to the effects on spacecraft instruments and the scattering of radar signals (Booker 1961; Jackson, Whale & Bauer 1962; Bernhardt 1987; Bernhardt *et al.* 1998, 2003; Ahmadov & Kunitsyn 2004; Bernhardt & Sulzer 2004; Bernhardt *et al.* 2011; Fu & Scales 2011; Bordikar & Scales 2012; Mahmoudian & Scales 2012). The launches of rockets and the exhausts of spacecraft engines accompany the combustion products into the atmosphere. These products usually contain both gas components and dispersed solid particles (Platov, Kulikova & Chernouss 2003; Platov, Chernouss & Kosch 2004). It is found that a dusty plasma is formed when electrons in the background plasma are attached to solid particles. Instabilities may arise because of the relative streaming of the dust to the background ionospheric plasma. Such instabilities might affect radar backscatter from the clouds, when the wave satisfies the Bragg condition for backscatter, $2k_r = k_w$, where k_r is the radar wavenumber and k_w is the wavenumber of the wave (Kelley & Heelis 2009).

The interaction between rocket exhausts and the background plasma has received growing interest owing to the potential role in the ionosphere (Fried & Conte 1963; Seiler, Yamada & Ikezi 1976; Shukla 1992; Mendis & Rosenberg 1994; Rosenberg & Krall 1994; Bernhardt *et al.* 1995; Bharuthram & Singh 1997; Bharuthram & Rosenberg 1998; Rosenberg, Salimullah & Bharuthram 1999; Huba, Joyce & Fedder 2000; Scales &

† Email addresses for correspondence: zhangheng@nwnu.edu.cn, duanws@nwnu.edu.cn

Ganguli 2004; Rosenberg & Sorasio 2006; Rosenberg, Bernhardt & Clark 2011; Bernhardt *et al.* 2012; Chen 2016; Liu *et al.* 2021). In a recent paper, Bernhardt *et al.* (1995) have studied possible mechanisms for enhanced radar backscatter from space shuttle exhaust in the ionosphere. It is found that ion acoustic waves and DAWs may be excited during this process. The enhancements in the backscatter from the radar signals are probably the result of scattering from these waves. Later, Bharuthram & Rosenberg (1998) used the parameters reported by Bernhardt *et al.* (1995) to study the generation of fluctuations by space shuttle exhaust in the ionosphere. It was found that instabilities may occur on the dust time scale. Subsequently, Rosenberg & Sorasio (2006) have investigated the lower hybrid instability driven by charged dust particles streaming across the geomagnetic field in the upper atmosphere and taken into account the effects of charged particles collisions with the background atmospheric molecules. It was found that the presence of unstable waves may create plasma density oscillations that could reflect radar signals. Bernhardt *et al.* (2012) have reported the ground and space-based measurement of rocket engine burns in the ionosphere. Although waves and instabilities driven by a charged dust beam in the ionosphere have been studied previously, the present paper chooses different altitudes in the ionosphere to study the wave modes excited by the relative streaming of the dust beam to the background plasma. It is found that different wave modes are excited in the ionosphere, whereas the chaotic behaviour appears on the dust particles vibration time scale. It seems that different wave modes and instabilities are excited at different altitudes, different times of the day and different seasons by relative streaming of the same dust beam to the background plasma in the ionosphere.

The paper is organised as follows. Section 2 gives the basic equations, and § 3 gives the dispersion relations of the waves for different frequency cases theoretically. The numerical simulation method and results are presented in §§ 4 and 5, respectively. Finally, § 6 gives the conclusion and discussion of the present paper.

2. Basic equation

In this paper, we consider a plasma consisting of electrons, singly charged ions, and negatively charged dust particles of the same size in a uniform magnetic field $\boldsymbol{B}_0 = B_0\boldsymbol{k}$, where $\boldsymbol{k}$ is the unit vector in the z-direction in the Cartesian coordinate system. We consider a case in which the propagation direction of the wave is in the x-direction, perpendicular to the direction of the magnetic field. Furthermore, for simplicity, we assume that the charged dust stream is in the same direction with speed u_{d0}. In an equilibrium state, both electrons and ions satisfy the Maxwell distribution, whereas the dust particles satisfy a drifting Maxwell distribution.

We now use the magnetohydrodynamic equations to study our system. The basic equations are as follows:

$$\frac{\partial n_d}{\partial t} + \nabla \cdot (n_d \boldsymbol{u}_d) = 0 \tag{2.1}$$

$$n_d m_d \left(\frac{\partial}{\partial t} + \boldsymbol{u}_d \cdot \nabla\right) \boldsymbol{u}_d = -\nabla p_d + n_d Q_d \boldsymbol{E} \tag{2.2}$$

$$\frac{\partial n_i}{\partial t} + \nabla \cdot (n_i \boldsymbol{u}_i) = 0 \tag{2.3}$$

$$n_i m_i \left(\frac{\partial}{\partial t} + \boldsymbol{u}_i \cdot \nabla\right) \boldsymbol{u}_i = -\nabla p_i + n_i Q_i \left(\boldsymbol{E} + \frac{\boldsymbol{u}_i \times \boldsymbol{B}}{c}\right) \tag{2.4}$$

https://doi.org/10.1017/S0022377822000058 Published online by Cambridge University Press

$$\frac{\partial n_e}{\partial t} + \nabla \cdot (n_e \boldsymbol{u}_e) = 0 \tag{2.5}$$

$$n_e m_e \left(\frac{\partial}{\partial t} + \boldsymbol{u}_e \cdot \nabla\right) \boldsymbol{u}_e = -\nabla p_e + n_e Q_e \left(\boldsymbol{E} + \frac{\boldsymbol{u}_e \times \boldsymbol{B}}{c}\right) \tag{2.6}$$

$$\nabla^2 \phi = -\frac{1}{\varepsilon_0}(n_d Q_d + n_i Q_i + n_e Q_e), \tag{2.7}$$

where n_α, $\boldsymbol{u}_\alpha$, m_α and Q_α are the number density, velocity, mass and charge of the species α ($\alpha = d, i, e$, denote the dust particles, ions and electrons), respectively. Here p_α is the pressure of species α ($\alpha = d, i, e$), and $\boldsymbol{E}$, $\boldsymbol{B}$, c and ϕ are the electric field, magnetic field, light velocity and electric potential, respectively. We use ε_0 to denote the permittivity of the vacuum. The charges on the dust particles are assumed to be constant due to the charging time of the dust particles being far less than the hydrodynamic time of the dust particles, i.e. $Q_d = \text{const}$.

3. Dispersion relation

In order to obtain the dispersion relation of the system, we assume that all the physical quantities vary in the following forms: $f = f_0 + f_1 \exp(\mathrm{i}(\boldsymbol{k} \cdot \boldsymbol{r} - \omega t))$, where f_0 is the value at its equilibrium state, f_1 is its small perturbation, $\boldsymbol{k}$ and ω are the wavenumber and frequency of the perturbation wave, respectively. We assume that $\boldsymbol{k}$ is in the xoz plane, i.e. a two-dimensional system, and the angle with the z-axis is θ, i.e. $\boldsymbol{k} = k_\perp \hat{x} + k_\parallel \hat{z} = k \sin\theta \hat{x} + k \cos\theta \hat{z}$, where $k = \mid \boldsymbol{k} \mid$. Then, we have from (2.1)–(2.7) the following dispersion relation:

$$1 - \frac{\omega_{\mathrm{pe}}^2 \left(1 + \dfrac{\Omega_{\mathrm{ce}}^2 \sin^2\theta}{\omega^2 - \Omega_{\mathrm{ce}}^2}\right)}{\omega^2 - k^2 \upsilon_e^2 \left(1 + \dfrac{\Omega_{\mathrm{ce}}^2 \sin^2\theta}{\omega^2 - \Omega_{\mathrm{ce}}^2}\right)} - \frac{\omega_{\mathrm{pi}}^2 \left(1 + \dfrac{\Omega_{\mathrm{ci}}^2 \sin^2\theta}{\omega^2 - \Omega_{\mathrm{ci}}^2}\right)}{\omega^2 - k^2 \upsilon_i^2 \left(1 + \dfrac{\Omega_{\mathrm{ci}}^2 \sin^2\theta}{\omega^2 - \Omega_{\mathrm{ci}}^2}\right)} - \frac{\omega_{\mathrm{pd}}^2}{(\omega - k \sin\theta u_{d0})^2 - k^2 \upsilon_d^2} = 0, \tag{3.1}$$

where $\omega_{p\alpha}$, $\Omega_{c\alpha}$ and υ_α are the oscillation frequency, cyclotron frequency and the thermal velocity of the species α ($\alpha = d, i, e$), respectively, $\omega_{p\alpha} = (n_\alpha e^2/\varepsilon_0 m_\alpha)^{1/2}$, $\Omega_{c\alpha} = (Q_\alpha B_0/m_\alpha)^{1/2}$ and $\upsilon_\alpha = (\gamma T_\alpha/m_\alpha)^{1/2}$. Here T_α is the temperature of the species α ($\alpha = d, i, e$).

Equation (3.1) is the dispersion relation of the linear wave for our system. In order to further understand it, we consider three special cases in the following because the masses of electrons, ions and dust particles in a dusty plasma are different widely, thus their oscillation frequencies are much different.

3.1. *High-frequency case*

First, we consider the high-frequency case: $\omega^2 > \omega_{\mathrm{pe}}^2$, $\Omega_{\mathrm{ce}}^2 \gg \omega_{\mathrm{pi}}^2 > \Omega_{\mathrm{ci}}^2 \gg \omega_{\mathrm{pd}}^2$, then the dispersion relation becomes as follows:

$$\omega^2 = (\omega_{\mathrm{pe}}^2 + k^2 \upsilon_e^2) \left(1 + \frac{\Omega_{\mathrm{ce}}^2 \sin^2\theta}{\omega^2 - \Omega_{\mathrm{ce}}^2}\right). \tag{3.2}$$

If the waves propagate in the direction parallel to the magnetic field, we have the dispersion relation of the Langmuir waves (LWs)

$$\omega^2 = \omega_{\mathrm{LM}}^2 = \omega_{\mathrm{pe}}^2 + k^2 \upsilon_e^2. \tag{3.3}$$

https://doi.org/10.1017/S0022377822000058 Published online by Cambridge University Press

If the waves propagate in the direction perpendicular to the magnetic field, we have the dispersion relation of the upper hybrid waves (UHWs)

$$\omega^2 = \omega_{\rm UH}^2 = \omega_{\rm pe}^2 + \Omega_{\rm ce}^2 + k^2\upsilon_e^2. \tag{3.4}$$

3.2. *Medium-frequency case*

Second, we consider the medium-frequency case: $\omega_{\rm pe}^2,\ \Omega_{\rm ce}^2 \gg \omega^2 > \omega_{\rm pi}^2 > \Omega_{\rm ci}^2 \gg \omega_{\rm pd}^2$, then the dispersion relation becomes as follows:

$$1 - \frac{\omega_{\rm pe}^2}{k^2\upsilon_e^2} - \frac{\omega_{\rm pi}^2\left(1 + \dfrac{\Omega_{\rm ci}^2\sin^2\theta}{\omega^2 - \Omega_{\rm ci}^2}\right)}{\omega^2 - k^2\upsilon_i^2\left(1 + \dfrac{\Omega_{\rm ci}^2\sin^2\theta}{\omega^2 - \Omega_{\rm ci}^2}\right)} = 0. \tag{3.5}$$

If the waves propagate in the direction parallel to the magnetic field, we have the dispersion relation of the dust ion acoustic waves (DIAWs)

$$\omega^2 = \omega_{\rm DIA}^2 = \frac{\omega_{\rm pi}^2 k^2\upsilon_e^2}{k^2\upsilon_e^2 + \omega_{\rm pe}^2} + k^2\upsilon_i^2. \tag{3.6}$$

If the waves propagate in the direction perpendicular to the magnetic field, we have the dispersion relation of the dust ion cyclotron waves (DICWs)

$$\omega^2 = \omega_{\rm DIC}^2 = \frac{\omega_{\rm pi}^2 k^2\upsilon_e^2}{k^2\upsilon_e^2 + \omega_{\rm pe}^2} + k^2\upsilon_i^2 + \Omega_{\rm ci}^2. \tag{3.7}$$

3.3. *Low-frequency case*

Finally, we consider the low-frequency case: $\omega_{\rm pe}^2,\ \Omega_{\rm ce}^2 \gg \omega_{\rm pi}^2 > \Omega_{\rm ci}^2 \gg \omega_{\rm pd}^2 > \omega^2$, the dispersion relation becomes as follows:

$$1 - \frac{\omega_{\rm pe}^2}{k^2\upsilon_e^2} - \frac{\omega_{\rm pi}^2}{k^2\upsilon_i^2} - \frac{\omega_{\rm pd}^2}{(\omega - k\sin\theta u_{d0})^2 - k^2\upsilon_d^2} = 0. \tag{3.8}$$

If the waves propagate in the direction parallel to the magnetic field, we have the following dispersion relation of the dust acoustic waves (DAWs)

$$\omega^2 = \omega_{\rm DA}^2 = \frac{k^2\omega_{\rm pd}^2}{k^2 + K_{\rm De}^2 + K_{\rm Di}^2} + k^2\upsilon_d^2. \tag{3.9}$$

If the waves propagate in the direction perpendicular to the magnetic field, we have

$$\omega = \omega_{\rm DAU} = \left(\frac{k^2\omega_{\rm pd}^2}{k^2 + K_{\rm De}^2 + K_{\rm Di}^2} + k^2\upsilon_d^2\right)^{1/2} + ku_{d0}, \tag{3.10}$$

where $K_{\rm De} = 1/\lambda_{\rm De}$, $K_{\rm Di} = 1/\lambda_{\rm Di}$, $\lambda_{\rm De}$ and $\lambda_{\rm Di}$ are the Debye length of the electrons and ions, respectively.

Figure 1 shows the dispersion relations given by (3.1) for our system. The dispersion relations on three different time scales are also shown in figure 1. Note that they are in agreement for small-wavenumber cases.

https://doi.org/10.1017/S0022377822000058 Published online by Cambridge University Press

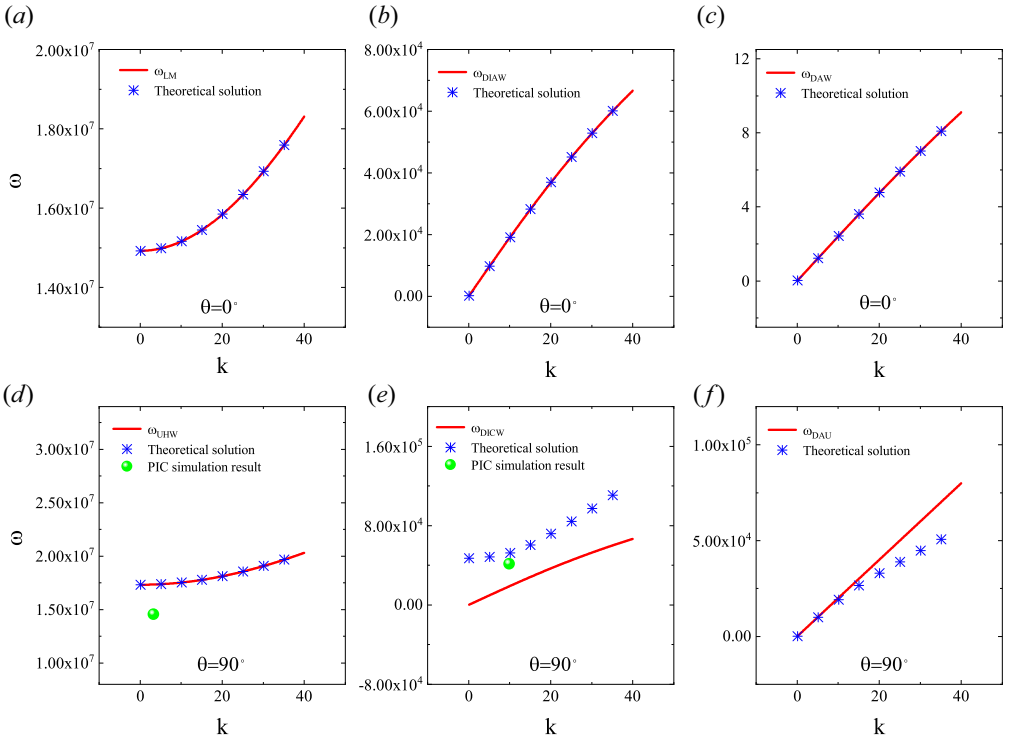

FIGURE 1. The dispersion relations of the waves excited by the relative streaming of the dust fluid to the background plasma, where the blue asterisks represent theoretical solutions of (3.1), the red solid lines represent the dispersion relations of the waves on three different time scales, and the green dots in (*d*) and (*e*) represent the particle-in-cell (PIC) simulation results on electron and ion vibration time scales, respectively.

4. Particle-in-cell simulation

We now investigate waves and instabilities driven by a charged dust beam in the ionosphere by using the particle-in-cell (PIC) simulation method. The initial condition is the equilibrium state of the system. The periodic boundary condition is used. We only study the motion of the dusty plasma in the *xoz* plane, i.e. a two-dimensional system. The size of the simulation area is 1902 mm × 951 mm, and 256 × 128 grid nodes are chosen. The equations of motion of the super particles (SPs) are the Newton equations as follows:

$$m_\alpha \frac{\mathrm{d}\boldsymbol{v}_\alpha}{\mathrm{d}t} = q_\alpha(\boldsymbol{E} + \boldsymbol{v}_\alpha \times \boldsymbol{B}), \tag{4.1}$$

$$\frac{\mathrm{d}\boldsymbol{r}_\alpha}{\mathrm{d}t} = \boldsymbol{v}_\alpha, \tag{4.2}$$

where m_α, q_α, $\boldsymbol{v}_\alpha$ and $\boldsymbol{r}_\alpha$ are the mass, charge, velocity and position of the species α ($\alpha = d, i, e$), respectively. Here $\boldsymbol{E}$ is the electric field and $\boldsymbol{B}$ is the external magnetic field. In the PIC simulation, the simulation area is divided into grid cells. At each time step, the velocities and the positions of SPs are weighted to all the grids to calculate the charge density ρ_g. Once ρ_g is obtained, the Poisson equation (electrostatic model) will be used to solve the potential of each grid, and the value of $\boldsymbol{E}$ is further derived. Then, each SP will be driven by the electric field according to (4.1) and (4.2), which will be

https://doi.org/10.1017/S0022377822000058 Published online by Cambridge University Press

solved numerically via the leap-frog algorithm. Finally, the new positions and velocities are obtained, the procedure repeats until the simulation is completed. As the masses of electrons, ions and dust particles vary widely, we choose different time steps and time scales for the simulations. The simulation is carried out for collisional and collisionless plasma, respectively.

First, on the electron vibration time scale, electrons, ions and dust particles in the plasma are treated as SPs. As the ion mass is much larger than the electron mass ($m_i/m_e \geqslant 1836$), as a first-order approximation, we assume that ions do not move, and only form a uniform background in space. The dust particles also do not move. We only study the oscillation of electrons. The parameters in the simulation are selected as follows: the space step is $\mathrm{d}x = \mathrm{d}z = \lambda_{\mathrm{Di}}$, $\lambda_{\mathrm{Di}} \sim 7.43 \times 10^{-3}$ m, the time step is $\mathrm{d}t = 2.0 \times 10^{-10}$ s.

Second, on the ion vibration time scale, electrons, ions and dust particles in the plasma are treated as SPs. The parameters in the simulation are selected as follows: the space step is $\mathrm{d}x = \mathrm{d}z = \lambda_{\mathrm{Di}}$, $\lambda_{\mathrm{Di}} \sim 7.43 \times 10^{-3}$ m, the time step is $\mathrm{d}t = 2.0 \times 10^{-8}$ s.

Third, on the dust vibration time scale, dust particles are regarded as SPs with macroscopic drift velocity, whereas electrons and ions are modelled as a Boltzmann distributed background. The parameters in the simulation are selected as follows: the space step is $\mathrm{d}x = \mathrm{d}z = \lambda_{\mathrm{Di}}$, $\lambda_{\mathrm{Di}} \sim 7.43 \times 10^{-3}$ m, the time step is $\mathrm{d}t = 2.0 \times 10^{-6}$ s.

In addition, we have considered the collision effects between particles on the waves in the system. We use the Monte Carlo method to study the collision between ions and neutrals, dust particles and neutrals. We neglect the collision between electrons and neutrals because the collisional frequency is so small compared with the electron oscillation frequency that can be ignored.

5. Numerical simulation results

We consider the F-region of the ionosphere at 240 km altitude. The primary ion in the F-region is O^+. The parameters chosen in the simulation are as follows: $B \sim 5 \times 10^{-5}$ T, $n_e \sim 0.994 \times 10^5$ cm^{-3}, $n_i \sim 1.0 \times 10^5$ cm^{-3}, $n_d \sim 0.006 n_i$, $T_e \sim 0.2$ eV, $T_d = T_i \sim 0.1$ eV, $Z_d \sim 50$ and $m_d \sim 4 \times 10^9 m_p$, where m_p is the proton mass (Mendis & Rosenberg 1994). The dust particles are injected into the background plasma with a speed $u_{d0} \sim 2$ km s^{-1} (Huba *et al.* 2000; Rosenberg & Sorasio 2006). Then we obtain $\omega_{\mathrm{pe}} = 1.50 \times 10^7$ rad s^{-1}, $\omega_{\mathrm{pi}} = 0.93 \times 10^5$ rad s^{-1}, $\omega_{\mathrm{pd}} = 25.50$ rad s^{-1}, $\Omega_{\mathrm{ce}} = 8.79 \times 10^6$ rad s^{-1}, $\Omega_{\mathrm{ci}} = 0.24 \times 10^3$ rad s^{-1} and $\Omega_{\mathrm{cd}} = 5.99 \times 10^{-5}$ rad s^{-1}.

Figure 2 shows the numerical results of the waves excited by the charged dust beam on the electron vibration time scale. The dependence of the electrostatic potential on time at the fixed point for collisionless dusty plasma is shown in figure 2(*a*), and its corresponding frequency spectrum analysis is given by figure 2(*b*). It seems from figures 2(*a*) and 2(*b*) that there is only one mode of the electron vibration and its frequency is about $\omega_e \sim 1.46 \times 10^7$ rad s^{-1}. In order to know what kind of wave is excited by this electron vibration, the variation of the electrostatic potential with the position is shown in figure 2(*c*), and its corresponding wavenumber spectrum analysis is given by figure 2(*d*). Note from figures 2(*c*) and 2(*d*) that the wavenumber is about $k_e \sim 3.28979$ m^{-1}. It is inferred from our numerical results of both wave frequency and wavenumber that the UHW is excited in the system by comparing our numerical results with the theoretical results in figure 1.

For collisional dusty plasma, the dependence of the electrostatic potential on time at the fixed point is shown in figure 2(*e*), and its corresponding spectrum analysis is given by figure 2(*f*). The variation of the electrostatic potential with the position is shown in figure 2(*g*), and its corresponding wavenumber spectrum analysis is given by figure 2(*h*).

https://doi.org/10.1017/S0022377822000058 Published online by Cambridge University Press

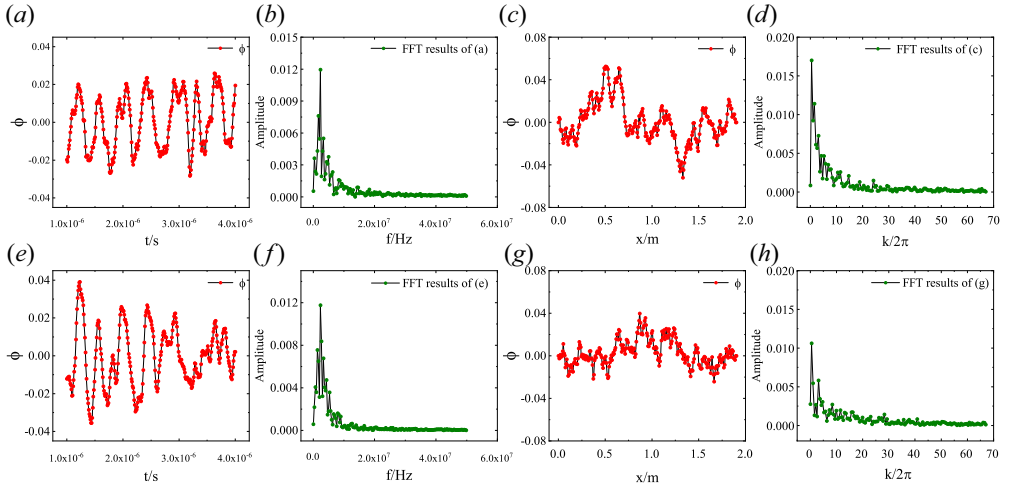

FIGURE 2. Numerical results of the electron vibration for (*a*)–(*d*) collisionless dusty plasma and (*e*)–(*h*) collisional dusty plasma. The dependence of the electrostatic potential on time is shown in (*a*) and (*e*) and the corresponding frequency spectrum is shown in (*b*) and (*f*). The variation of the electrostatic potential with respect to the position is shown in (*c*) and (*g*) and the corresponding frequency spectrum is shown in (*d*) and (*h*).

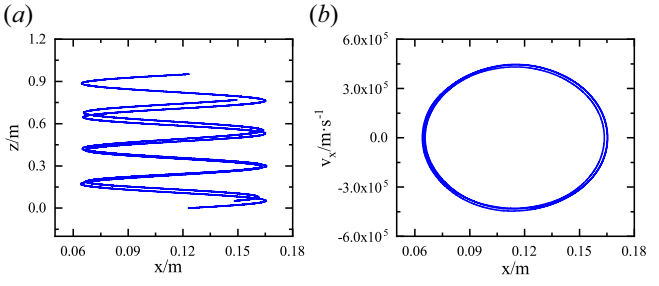

FIGURE 3. (*a*) The trajectory of one of the SPs in the *xoz* plane. (*b*) The phase diagram of the SP in phase space of (x, υ_x).

Numerical results show that the effects of the collision between electrons and neutrals can be neglected because the collision frequency between electrons and neutrals is much smaller than the vibration frequency of the electrons.

In order to investigate whether this wave is stable, the trajectory and phase diagram of a single SP (electron) are given in figure 3. It seems that the wave is quasi-periodic. Therefore, it is stable.

Figure 4 shows the numerical results of the waves excited by the charged dust beam on the ion vibration time scale. The dependence of the electrostatic potential on time at the fixed point for collisionless dusty plasma is shown in figure 4(*a*), and its corresponding spectrum analysis is given by figure 4(*b*). It seems from figures 4(*a*) and 4(*b*) that there is only one mode of the ion vibration, and its frequency is about $\omega_i \sim 4.17 \times 10^4$ rad s^{-1}. In order to know what kind of wave is excited by this ion vibration, the variation of the electrostatic potential with the position is shown in figure 4(*c*), and its corresponding spectrum analysis is given by figure 4(*d*). Note from figures 4(*c*) and 4(*d*) that the wavenumber is about $k \sim 9.87$ m^{-1}. It is inferred from our numerical results of both wave

https://doi.org/10.1017/S0022377822000058 Published online by Cambridge University Press

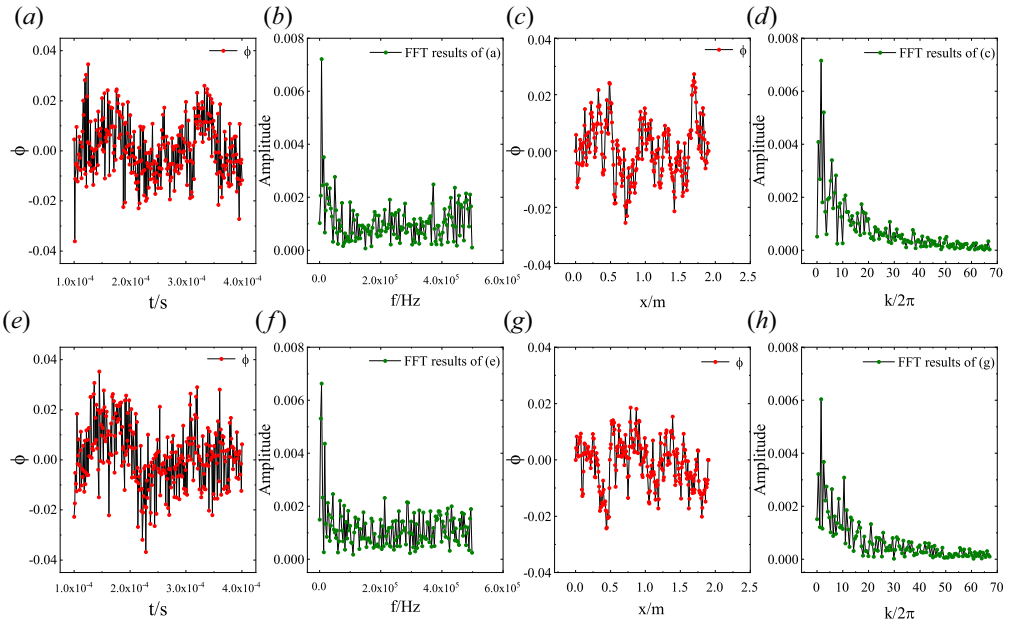

FIGURE 4. Numerical results of the ion vibration for (*a*)–(*d*) collisionless dusty plasma and (*e*)–(*h*) collisional dusty plasma. The dependence of the electrostatic potential on time is shown in (*a*) and (*e*) and the corresponding frequency spectrum is shown in (*b*) and (*f*). The variation of the electrostatic potential with respect to the position is shown in (*c*) and (*g*) and the corresponding frequency spectrum is shown in (*d*) and (*h*).

frequency and wavenumber that the DICW is excited in the system by comparing our numerical results with the theoretical results in figure 1.

For collisional dusty plasma, the dependence of the electrostatic potential on time at the fixed point is shown in figure 4(*e*), and its corresponding spectrum analysis is given by figure 4(*f*). The variation of the electrostatic potential with the position is shown in figure 4(*g*), and its corresponding spectrum analysis is given by figure 4(*h*). It seems from the numerical results that the collisional effect on the ion vibration time scale is so small that it is negligible.

In order to know whether the ion vibration is stable or not, we give the Lyapunov index in table 1. It is noted that the Lyapunov indexes are all negative. Therefore, we conclude that the wave on the ion vibration time scale may be stable no matter the collisions between particles are considered or not.

Figure 5 shows the numerical results of the waves excited by the charged dust beam on the dust vibration time scale. The dependence of the electrostatic potential on time at the fixed point for collisionless dusty plasma is shown in figure 5(*a*), and its corresponding spectrum analysis is given by figure 5(*b*). For the collisional dusty plasma, the variation of the electrostatic potential with the time at the fixed point is shown in figure 5(*c*), and its corresponding spectrum analysis is given by figure 5(*d*).

Note from figures 5(*a*)–5(*d*) that the modes of the dust vibration are more complex. There is no certain frequency of the vibration of dust particles for both collisional and collisionless dusty plasma. Therefore, we now focus on whether the waves excited by the dust fluid beam on the dust particles vibration time scale are stable or not. For this purpose, the corresponding Lyapunov index of the dust vibration is listed in table 2. It is found

https://doi.org/10.1017/S0022377822000058 Published online by Cambridge University Press

Super particles	No collision	Collision
1600	−1838.79	−932.16
3400	−2814.37	−1442.58
5800	−5829.47	−1030.25
6000	−288.38	−342.20
6300	−2193.63	−574.54
6600	−9366.56	−72.33
7200	−597.08	−2868.91
7500	−1878.87	−2436.02
7980	−5904.81	−1871.80
8000	−2331.05	−889.40
8500	−2433.60	−164.45
9600	−309.63	−1897.18
9900	−4753.60	−1123.62
11 600	−1210.81	−1246.25
10 230	−3027.18	−558.29
13 200	−2099.32	−514.68
16 000	−2293.84	−2873.87
100 000	−295.07	−1629.92
160 000	−1077.05	−8955.51
1 250 000	−4378.37	−318.67

TABLE 1. The Lyapunov index on the ion vibration time scale.

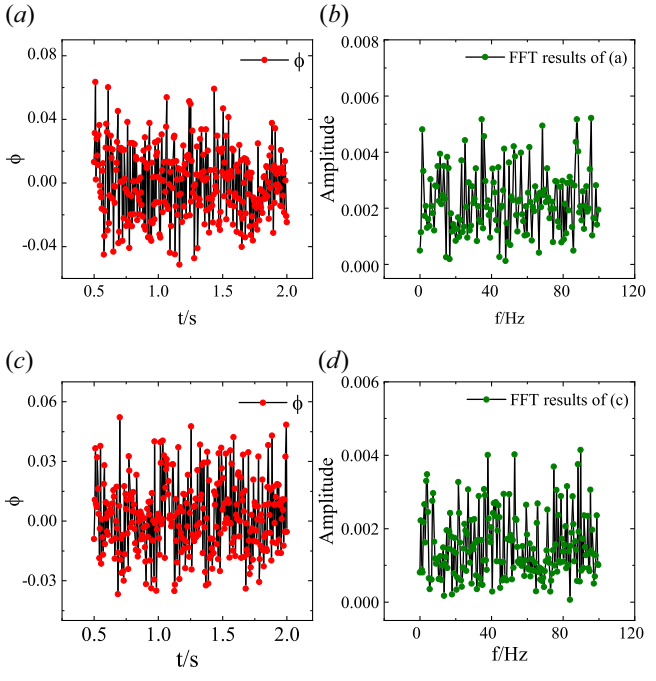

FIGURE 5. Numerical results of the vibration of the dust particles for (*a*) and (*b*) collisionless dusty plasma and (*c*) and (*d*) collisional dusty plasma. The dependence of the electrostatic potential on time is shown in (*a*) and (*c*), and the corresponding frequency spectrum is shown in (*b*) and (*d*).

https://doi.org/10.1017/S0022377822000058 Published online by Cambridge University Press

Super particles	No collision	Collision
1600	−0.78	−0.23
3400	−0.36	−0.05
5800	−0.03	0.02
6000	0.09	−0.04
6300	−1.32	0.96
6600	1.01	−0.22
7200	−0.43	−0.37
7500	−0.18	−0.01
7980	0.02	2.03
8000	0.07	0.30
8500	0.08	−0.18
9600	0.08	−0.07
9900	0.32	−0.35
11 600	−0.35	0.18
10 230	−0.51	−0.02
13 200	−0.41	0.05
16 000	0.77	−0.42
100 000	0.42	−0.55
160 000	−0.73	−0.94
1 250 000	0.45	−0.02

TABLE 2. The Lyapunov index on the dust particles vibration time scale.

that the Lyapunov indexes of the dust vibration always have positive values no matter the collisions between particles are considered or not. We then conclude that the vibrations on the dust particles time scale are unstable.

6. Discussion and conclusion

In this paper, we have studied the waves and instabilities excited by the relative streaming of the dust beam to the background plasma in the F-region of the ionosphere at 240 km altitude by using the PIC simulation method. The dispersion relations for this system have been obtained. Different wave frequencies have been obtained on different time scales of the electron vibration, the ion vibration and the dust particle vibration. Furthermore, the differences of the wave frequencies in different wave propagation directions have also been studied.

It has been found from our numerical results that there are a stable UHW which is on the electron vibration time scale and a stable DICW on the ion vibration time scale. However, waves excited by dust particles vibration are unstable. The chaotic behaviour occurs on the dust particles vibration time scale due to the relative streaming of the dust particles to the background plasma.

The present paper shows that unstable DAWs are excited by the relative streaming of dust beam to the background plasma. These instabilities may drive plasma irregularities that could affect radar backscatter from the clouds. Modifications in the backscatter of the radar were experimentally recorded in the ionosphere (Bernhardt *et al.* 1995; Bharuthram & Rosenberg 1998; Rosenberg *et al.* 1999; Huba *et al.* 2000; Scales & Ganguli 2004; Rosenberg *et al.* 2011; Bernhardt *et al.* 2012). The modifications in the backscatter are possibly the results of the excitation of DAWs and ion acoustic waves. The radar echoes are also probably modified due to the scatter from these waves. Therefore, present results

https://doi.org/10.1017/S0022377822000058 Published online by Cambridge University Press

may have potential applications in atmospheric science. For example, by measuring the wave modes excited by the dust beam to the background plasma in the ionosphere, we can estimate the altitude and the time of the rocket exhaust.

Acknowledgements

This work was supported by the National Natural Science Foundation of China (grant numbers 11965019, 42004131, 61863032 and 42065005).

Editor Edward Thomas, Jr. thanks the referees for their advice in evaluating this article.

Declaration of interests

The authors report no conflicts of interest.

REFERENCES

AHMADOV, R.R. & KUNITSYN, V.E. 2004 Simulation of generation and propagation of acoustic gravity waves in the atmosphere during a rocket flight. *Intl J. Geomagnet. Aeronomy* **5**, GI2002.

BERNHARDT, P.A. 1987 A critical comparison of ionospheric depletion chemicals. *J. Geophys. Res*. **92** (A5), 4617–4628.

BERNHARDT, P.A., BALLENTHIN, J.O., BAUMGARDNER, J.L., BHATT, A., BOYD, I.D., BURT, J.M., CATON, R.G., COSTER, A., ERICKSON, P.J., HUBA, J.D., *et al.* . 2012 Ground and space-based measurement of rocket engine burns in the ionosphere. *IEEE Trans. Plasma Sci*. **40** (5), 1267–1286.

BERNHARDT, P.A., BAUMGARDNER, J.B., BHATT, A.N., ERICKSON, P.J., LARSEN, M.F., PEDERSEN, T.R. & SIEFRING, C.L. 2011 Optical emissions observed during the charged aerosol release experiment (CARE I) in the ionosphere. *IEEE Trans. Plasma Sci*. **39** (11), 2774–2775.

BERNHARDT, P.A., ERICKSON, P.J., LIND, F.D., FOSTER, J.C. & REINISCH, B. 2003 Artificial disturbances of the ionosphere over the Millstone Hill radar during dedicated burns of the space shuttle OMS engines. In *AIAA Space 2003 Conference and Exposition*. American Institute of Aeronautics and Astronautics.

BERNHARDT, P.A., GANGULI, G., KELLEY, M.C. & SWARTZ, W.E. 1995 Enhanced radar backscatter from space shuttle exhaust in the ionosphere. *J. Geophys. Res*. **100** (A12), 23811–23818.

BERNHARDT, P.A., HUBA, J.D., SWARTZ, W.E. & KELLEY, M.C. 1998 Incoherent scatter from space shuttle and rocket engine plumes in the ionosphere. *J. Geophys. Res*. **103** (A2), 2239–2251.

BERNHARDT, P.A. & SULZER, M.P. 2004 Incoherent scatter measurements of ring-ion beam distributions produced by space shuttle exhaust injections into the ionosphere. *J. Geophys. Res*. **109**, A02303.

BHARUTHRAM, R. & ROSENBERG, M. 1998 A note on the generation of fluctuations by space shuttle exhaust in the ionosphere. *Planet. Space Sci*. **46** (4), 425–427.

BHARUTHRAM, R. & SINGH, S.V. 1997 Lower hybrid drift instability in dusty plasmas. *Phys. Scr*. **55**, 345–349.

BOOKER, H.G. 1961 A local reduction of F-region ionization due to missile transit. *J. Geophys. Res*. **66** (4), 1073–1079.

BORDIKAR, M.R. & SCALES, W. 2012 Lower hybrid turbulence associated with creation of dusty plasmas in the near-Earth space environment. *IEEE Trans. Plasma Sci*. **40** (3), 946–953.

CHEN, F.F. 2016 *Introduction to Plasma Physics and Controlled Fusion*. Springer International Publishing, https://doi.org/10.1007/978-3-319-22309-4.

FRIED, B.D. & CONTE, S.D. 1963 The plasma dispersion function: The Hilbert transform of the Gaussian. *Math. Comput.* **17** (81), 94–95.

FU, H. & SCALES, W.A. 2011 Nonlinear evolution of the ion acoustic instability in artificially created dusty space plasmas. *J. Geophys. Res*. **116**, A10315.

HUBA, J.D., JOYCE, G. & FEDDER, J.A. 2000 SAMI2 is another model of the ionosphere (SAMI2): a new low-latitude ionosphere model. *J. Geophys. Res*. **105** (A10), 23035–23053.

JACKSON, J.E., WHALE, H.A. & BAUER, S.J. 1962 Local ionospheric disturbance created by a burning rocket. *J. Geophys. Res*. **67** (5), 2059–2061.

KELLEY, M.C. & HEELIS, R.A. 2009 *The Earth's Ionosphere: Plasma Physics and Electrodynamics*, 2nd edn. Academic Press (Elsevier).

LIU, B., HAN, J.F., XU, B., LI, H. & DUAN, W.S. 2021 The instability of the waves driven by a charged dust beam in the ionosphere. *Mod. Phys. Lett.* B **35** (14), 2150243.

MAHMOUDIAN, A. & SCALES, W.A. 2012 Irregularity excitation associated with charged dust cloud boundary layers. *J. Geophys. Res*. **117**, A02304.

MENDIS, D.A. & ROSENBERG, M. 1994 Cosmic dusty plasma. *Annu. Rev. Astron. Astrophys*. **32**, 419–463.

PLATOV, Y.V., CHERNOUSS, S.A. & KOSCH, M.J. 2004 Classification of gas-dust formations from rocket exhaust in the upper atmosphere. *J. Spacecr. Rockets* **41** (4), 667–670.

PLATOV, Y.V., KULIKOVA, G.N. & CHERNOUSS, S.A. 2003 Classification of gas-dust structures in the upper atmosphere associated with the exhausts of rocket-engine combustion products. *Cosmic Res*. **41** (2), 153–158.

ROSENBERG, M., BERNHARDT, P.A. & CLARK, S.E. 2011 Excitation of ion waves by charged dust beams in ionospheric aerosol release experiments. *Planet. Space Sci*. **59**, 312–318.

ROSENBERG, M. & KRALL, N.A. 1994 High frequency drift instabilities in a dusty plasma. *Planet. Space Sci*. **42** (10), 889–894.

ROSENBERG, M., SALIMULLAH, M. & BHARUTHRAM, R. 1999 Lower hybrid instability driven by charged dust beam. *Planet. Space Sci*. **47**, 1517–1519.

ROSENBERG, M. & SORASIO, G. 2006 Lower hybrid instability in ionospheric gas-dust formations from rocket exhaust. *J. Spacecr. Rockets* **43** (1), 245–247.

SCALES, W.A. & GANGULI, G. 2004 Electrodynamic structure of charged dust clouds in the Earth's middle atmosphere. *New J. Phys*. **6** (12), 1–15.

SEILER, S., YAMADA, M. & IKEZI, H. 1976 Lower hybrid instability driven by a spiraling ion beam. *Phys. Rev. Lett*. **37** (11), 700–703.

SHUKLA, P.K. 1992 Low-frequency modes in dusty plasmas. *Phys. Scr*. **45**, 504–507.